
# Long-range angular correlations of charged particles in high multiplicity $e^+e^-$ collisions using archived data from the ALEPH detector at LEP

Anthony Badea, Austin Baty, Gian Michele Innocenti, Yen-Jie Lee,
Christopher McGinn, Bibek Pandit, Michael Peters, and Jesse Thaler
*Massachusetts Institute of Technology*

Paoti Chang and Tzu-An Sheng
*National Taiwan University*

Marcello Maggi
*Universita degli Studi di Bari*

(Dated: May 7, 2018)

## Abstract

First results on two-particle angular correlations for charged particles emitted in $e^+e^-$ collisions using 730 $pb^{-1}$ of data collected between 91 and 209 GeV with the ALEPH detector at LEP are presented. With the archived data, the correlation functions are studied over a broad range of pseudorapidity $\eta$ (rapidity $y$) and azimuthal angle $\phi$ with respect to the electron-positron beam axis and the event thrust axis. Short-range correlations in $\Delta\eta$ ($\Delta y$), which are studied with $e^+e^-$ annihilations which reveal jet-like correlations. Long-range azimuthal correlations are studied differentially as a function of charged particle multiplicity. Those results are compared to event generators and are complementary to the particle correlation analyses in high multiplicity proton-proton, proton-nucleus and nucleus-nucleus collisions at the RHIC and the LHC.

**CONTENTS**

## I. INTRODUCTION

This analysis note presents the measurements of two-particle angular correlations of charged hadrons produced in $e^+e^-$ collisions as a function of charged hadron multiplicity, using 730 $pb^{-1}$ of archived data collected between 91 and 209 GeV with the ALEPH detector at LEP. Two-particle correlations in high-energy collisions provide valuable information for characterizing Quantum Chromodynamics and have been studied previously for a broad range of collision energies in proton-proton (pp) [**?** ], proton-nucleus (pA) [**?** **?** **?** ], and nucleus-nucleus (AA) [**?** **?** ] collisions. Such measurements can elucidate the underlying mechanism of particle production and reveal possible collective effects resulting from the high particle densities accessible in these collisions.

Studies of two-particle angular correlations in pp, pA and AA collisions are typically performed using two-dimensional $\Delta\eta - \Delta\phi$ correlation functions, where $\Delta\phi$ is the difference in the azimuthal angle $\phi$ between the two particles and $\Delta\eta$ is the difference in pseudorapidity $\eta = -\ln(\tan(\theta/2))$. The polar angle $\theta$ is defined relative to the counterclockwise hadron beam direction.

Of particular interest in studies of collective effects is the long-range (large $|\Delta\eta|$) structure of the two-particle correlation functions. In this region, the function is less susceptible to other known sources of correlations such as resonance decays and fragmentation function of energetic jets. Measurements in high-energy AA collisions have shown significant modification of the long-range structure compared with minimum-bias pp collisions, over a very wide range of collision energies [**?** **?** **?** **?** ]. The long-range correlations are commonly interpreted as a consequence of the hydrodynamical flow of the produced strongly interacting medium [**?** ] and usually characterized by the Fourier components of the azimuthal particle distributions. The extraction of the second and third Fourier components, usually referred to as elliptic and triangular flow, is of great interest because it is closely related to initial collision geometry and its fluctuation [**?** ]. Those measurements allow the extraction of the fundamental transport properties of the medium using hydrodynamic models.

Recently, measurements in pp [**?** ] and pPb collisions [**?** **?** **?** ] have revealed the

emergence of long-range, near-side ($\Delta\phi \sim 0$) correlations in the selection of collisions with very high number of final state particles. This "ridge-like" correlation has inspired a large variety of theoretical models [**?** **?** ]. The physical origin of the phenomenon is not yet fully understood. Moreover, it was found that the elliptic flow signal exists even at the lowest nucleon-nucleon center-of-mass energy of 7.7 GeV in AA collisions at the Relativistic Heavy Ion Collider [**?** ].

Due to the complexity of the hadron-hadron collisions, possible initial state correlations of the partons, such as those arise from color-glass condensate [**?** **?** ], could complicate the interpretation of the pp and pA data. Studies of high multiplicity $e^+e^-$ collision, where the initial kinematics of the collisions are well-controlled, could bring significant insights about the observed phenomenon. These measurements will also enable a direct comparison between different collision systems for the first time. The studies of ridge signal in $e^+e^-$ collisions will bring significant impact to the field of relativistic heavy ion collisions, either change completely the interpretation of the ridge in pp, pA and AA collisions if a significant signal is observed, or serve as an important reference for the final state effect observed in high multiplicity hadron-hadron scatterings if no long-range correlation signal was detected.

With the archived data from ALEPH collaboration, the correlation functions are studied over a broad range of pseudorapidity $\eta$ (rapidity $y$) and azimuthal angle $\phi$ with respect to the electron-positron beam axis. In addition, the correlation functions are also studied using azimuthal and polar angles calculated with respect to the the event thrust axis and a dijet axis in order to follow the direction of the extending color strings.

## II. THE ALEPH DETECTOR

The central part of the ALEPH detector is dedicated to the reconstruction of charged particles, which are measured by a two-layer silicon strip vertex detector, a cylindrical drift chamber and a large time projection chamber. The three detectors are immersed in a 1.5 T axial magnetic field generated by a superconducting solenoid. Electrons and photons are identified in the electromagnetic calorimeter (ECAL), which is a sampling calorimeter sandwidch of lead plates and proportional wire chambers segmented in $0.9^\circ \times 0.9^\circ$ projective towers and read out in three sections in depth. The iron return yoke forms the hadron calorimeter (HCAL), which are used to measure the energy of charged and neutral hadrons.

Muons are distinguished from hadrons by HCAL and muon chambers, which consists of two double-layers of streamer tubes outside HCAL. Detailed description of the ALEPH detector and its performance could be found in **??**.

## III. DATA SAMPLE

The ALEPH archieved data used in this analysis will be documented in this section, which include both LEP1 and LEP2 period.

## IV. DATA QUALITY CHECKS

This section documents the basic data quality checks for ALEPH archieved data collected in the LEP1 and LEP2 period. In additional to the raw spectra from the data, jet and particle spectra are compared to the predictions from PYTHIA8 event generator (Version 8.230 Default Tune).

### A. LEP1 vs LEP1 Monte-Carlo

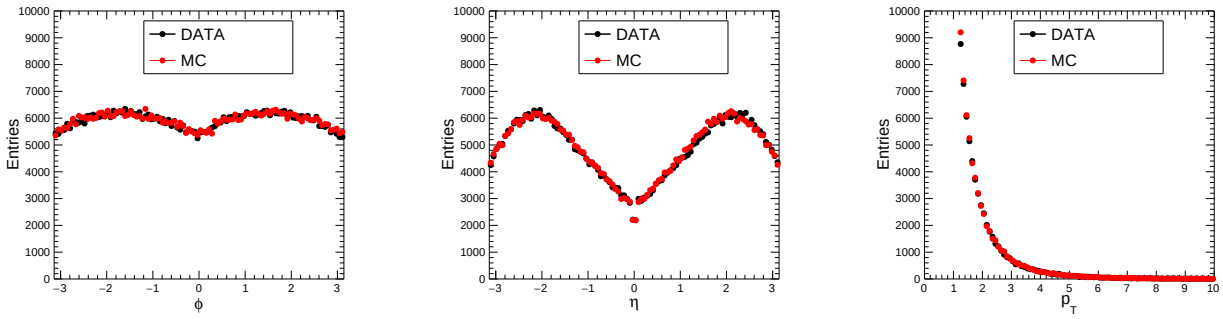


FIG. 1

## V. ANALYSIS

## VI. THRUST AND SPHERICITY AXES

The thrust $T$, and the thrust axis, $\hat{n}$, are defined as using the vector which maximizes the sum of the projection of the momenta of all particles in the event onto the axis:

$$T = max_{\hat{n}} \frac{\sum_i |\hat{p}_i.\hat{n}|}{\sum_i |\hat{p}_i|}. \quad (1)$$

Events which are 'pencil-like' in shape are expected to have $T$ close to unity, while events in which the particles are distributed rather isotropically are expected to have $T$ close to 0.5.

The thrust is calculated for an event having $n$ particles, each having a momentum $\vec{p_i}$, using an iterative procedure. The initial thrust axis, $\vec{T_0}$ is first taken to be a unit vector along the axis of any particle. The thrust axis is then updated according to

$$\vec{T_{i+1}} = \vec{T_i} + \sum_{j=1}^{n} \mathrm{sign}(\vec{\mathrm{p_j}} \cdot \vec{\mathrm{T_i}})\vec{\mathrm{p_j}}. \quad (2)$$

This procedure is repeated until there have either been $n$ iterations, or when the sign of $\vec{p_j} \cdot \vec{T_i}$ does not change for every particle between the $i$ and $i+1$ iterations. The resulting vector, $\vec{T}_{\mathrm{cand}}$, is then stored as a thrust axis candidate. The entire procedure is then repeated $n$ times, each time starting with a new initial particle, to give $n$ thrust axis candidates. The candidate which maximizes the quantity $T$ is then chosen as the final thrust axis.

Another event shape variable used in this analysis is the sphericity axis. The sphericity tensor is defined as

$$S^{\alpha\beta} = \frac{\sum\limits_i p_i^{\alpha} p_i^{\beta}}{\sum\limits_i |p_i|^2}, \quad (3)$$

where $\alpha$ and $\beta$ can take on values of one to three, corresponding to the $x$, $y$, and $z$ axes. This can be diagonalized and three eigenvalues, $\lambda_1 \geq \lambda_2 \geq \lambda_3$ can be found, whose sum is unity. The sphericity is defined as

$$S = \frac{3}{2}(\lambda_2 + \lambda_3). \quad (4)$$

It is bound between zero and one, with zero corresponding to a 'pencil-like' event and one corresponding to an isotropic event. A related variable, the Aplanarity is defined as

$$A = \frac{3}{2}(\lambda_3). \quad (5)$$

A planar event has $A = 0$, while an isotropic one has $A = 0.5$.

The sphericity axis, $\vec{S}$ is simply defined as the eigenvector corresponding to $\lambda_1$.

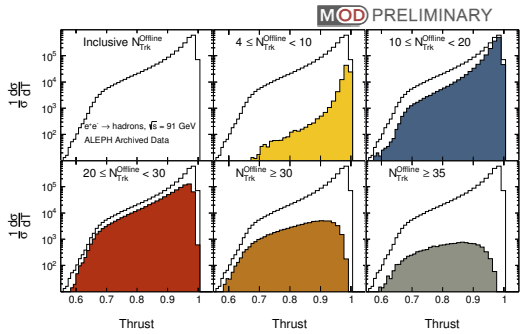


FIG. 2: Thrust distribution as a function of $N_{Trk}^{Offline}$ for archived ALEPH data

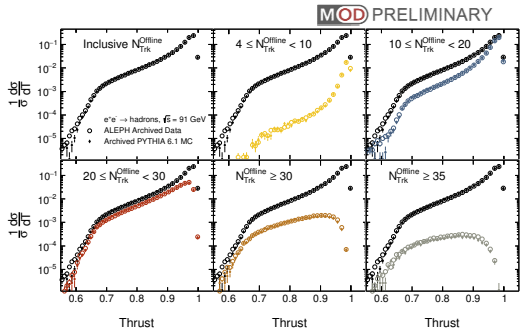


FIG. 3: Thrust distribution as a function of $N_{Trk}^{Offline}$ for archived ALEPH data and PYTHIA 6.1 Monte Carlo

## VII. EVENT SELECTION

## VIII. THRUST DISTRIBUTION

In order to validate the ALEPH archived data sample and our understanding, an analysis of the thrust distribution ($T$) is performed with LEP1 archived data. The distributions are corrected for the detector response by ALEPH MC produced in 1994. The results are unfolded by a Bayesian unfolding method. The size of the correction factor is small in the mid-$T$ and becomes larger as we go to smaller $T$ or larger $T$ regions.

Figure **??** shows the corrected thrust distribution from ALEPH archived data. The results are compared to ALEPH publications [**?** **?** ]. As shown in the figure, a very good agreement between ALEPH archived data from this note and ALEPH publications in the low $T$ region.

In the $T \sim 1$ region, a small difference at the level of 0-10% is observed between this work and the ALEPH publication in 2004 [**?** ]. This could be due to the difference in unfolding procedure, the dataset used and the event selection criteria.

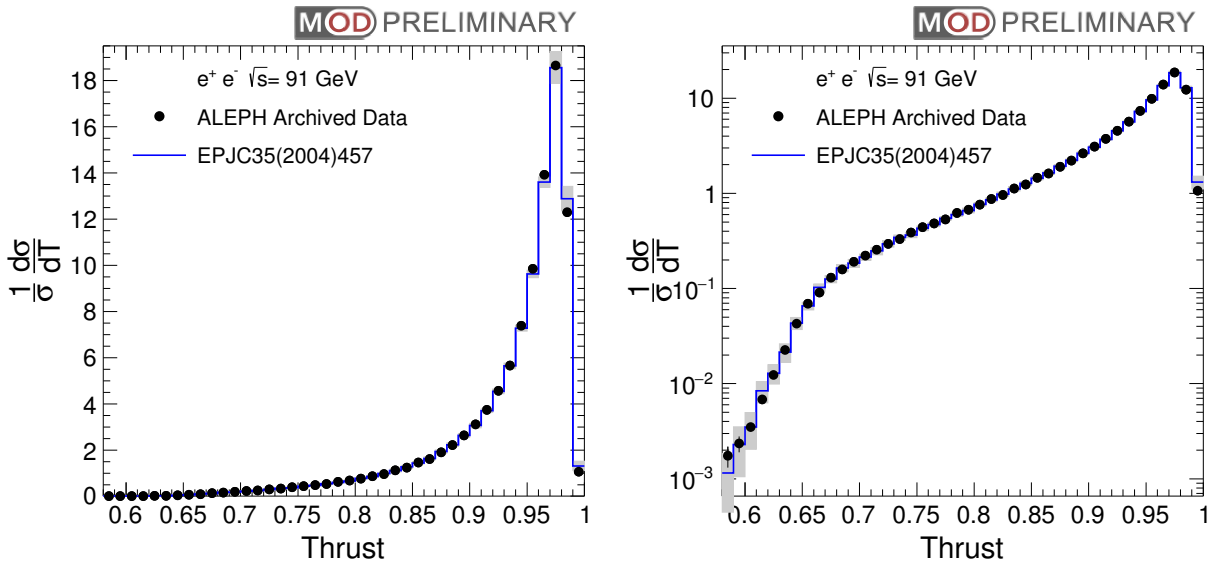


FIG. 4: The corrected thrust distribution from ALEPH archived data compared to previous publications in linear and log scale.


[1] CMS Collaboration, "Observation of Long-Range Near-Side Angular Correlations in Proton-Proton Collisions at the LHC", *JHEP* **09** (2010) 091, doi:10.1007/JHEP09(2010)091, arXiv:1009.4122.

[2] CMS Collaboration, "Observation of long-range near-side angular correlations in proton-lead collisions at the LHC", *Phys. Lett.* **B718** (2013) 795–814, doi:10.1016/j.physletb.2012.11.025, arXiv:1210.5482.

[3] ALICE Collaboration, "Long-range angular correlations on the near and away side in $p$-Pb collisions at $\sqrt{s_{NN}} = 5.02$ TeV", *Phys. Lett.* **B719** (2013) 29–41, doi:10.1016/j.physletb.2013.01.012, arXiv:1212.2001.

[4] ATLAS Collaboration, "Observation of Associated Near-Side and Away-Side Long-Range Correlations in $\sqrt{s_{NN}}$=5.02??TeV Proton-Lead Collisions with the ATLAS Detector",

*Phys. Rev. Lett.* **110** (2013), no. 18, 182302, doi:10.1103/PhysRevLett.110.182302, arXiv:1212.5198.

[5] ALICE Collaboration, "Elliptic flow of charged particles in Pb-Pb collisions at 2.76 TeV", *Phys. Rev. Lett.* **105** (2010) 252302, doi:10.1103/PhysRevLett.105.252302, arXiv:1011.3914.

[6] CMS Collaboration, "Centrality dependence of dihadron correlations and azimuthal anisotropy harmonics in PbPb collisions at $\sqrt{s_{NN}} = 2.76$ TeV", *Eur. Phys. J.* **C72** (2012) 2012, doi:10.1140/epjc/s10052-012-2012-3, arXiv:1201.3158.

[7] B. B. Back et al., "The PHOBOS perspective on discoveries at RHIC", *Nucl. Phys.* **A757** (2005) 28–101, doi:10.1016/j.nuclphysa.2005.03.084, arXiv:nucl-ex/0410022.

[8] BRAHMS Collaboration, "Quark gluon plasma and color glass condensate at RHIC? The Perspective from the BRAHMS experiment", *Nucl. Phys.* **A757** (2005) 1–27, doi:10.1016/j.nuclphysa.2005.02.130, arXiv:nucl-ex/0410020.

[9] PHENIX Collaboration, "Formation of dense partonic matter in relativistic nucleus-nucleus collisions at RHIC: Experimental evaluation by the PHENIX collaboration", *Nucl. Phys.* **A757** (2005) 184–283, doi:10.1016/j.nuclphysa.2005.03.086, arXiv:nucl-ex/0410003.

[10] STAR Collaboration, "Experimental and theoretical challenges in the search for the quark gluon plasma: The STAR Collaboration's critical assessment of the evidence from RHIC collisions", *Nucl. Phys.* **A757** (2005) 102–183, doi:10.1016/j.nuclphysa.2005.03.085, arXiv:nucl-ex/0501009.

[11] J.-Y. Ollitrault, "Anisotropy as a signature of transverse collective flow", *Phys. Rev.* **D46** (1992) 229–245, doi:10.1103/PhysRevD.46.229.

[12] B. Alver and G. Roland, "Collision geometry fluctuations and triangular flow in heavy-ion collisions", *Phys. Rev.* **C81** (2010) 054905, doi:10.1103/PhysRevC.82.039903, 10.1103/PhysRevC.81.054905, arXiv:1003.0194. [Erratum: Phys. Rev.C82,039903(2010)].

[13] A. Bzdak, B. Schenke, P. Tribedy, and R. Venugopalan, "Initial state geometry and the role of hydrodynamics in proton-proton, proton-nucleus and deuteron-nucleus collisions", *Phys. Rev.* **C87** (2013), no. 6, 064906, doi:10.1103/PhysRevC.87.064906, arXiv:1304.3403.

[14] K. Dusling, W. Li, and B. Schenke, "Novel collective phenomena in high-energy proton?proton and proton?nucleus collisions", *Int. J. Mod. Phys.* **E25** (2016), no. 01, 1630002, doi:10.1142/S0218301316300022, arXiv:1509.07939.

[15] STAR Collaboration, "Inclusive charged hadron elliptic flow in Au + Au collisions at $\sqrt{s_{NN}}$ = 7.7 - 39 GeV", *Phys. Rev.* **C86** (2012) 054908, doi:10.1103/PhysRevC.86.054908, arXiv:1206.5528.

[16] F. Gelis, E. Iancu, J. Jalilian-Marian, and R. Venugopalan, "The Color Glass Condensate", *Ann. Rev. Nucl. Part. Sci.* **60** (2010) 463–489, doi:10.1146/annurev.nucl.010909.083629, arXiv:1002.0333.

[17] K. Dusling and R. Venugopalan, "Comparison of the color glass condensate to dihadron correlations in proton-proton and proton-nucleus collisions", *Phys. Rev.* **D87** (2013), no. 9, 094034, doi:10.1103/PhysRevD.87.094034, arXiv:1302.7018.

[18] ALEPH Collaboration, "Studies of quantum chromodynamics with the ALEPH detector", *Phys. Rept.* **294** (1998) 1–165, doi:10.1016/S0370-1573(97)00045-8.

[19] ALEPH Collaboration, "Studies of QCD at e+ e- centre-of-mass energies between 91-GeV and 209-GeV", *Eur. Phys. J.* **C35** (2004) 457–486, doi:10.1140/epjc/s2004-01891-4.